

Structural characterization of metal-metal interfaces by intermediate-energy Auger-electron diffraction

S. A. Chambers

Department of Chemistry, Bethel College, St. Paul, Minnesota 55112

S. B. Anderson

Department of Physics, Bethel College, St. Paul, Minnesota 55112

J. H. Weaver

Department of Chemical Engineering and Materials Science, University of Minnesota, Minneapolis, Minnesota 55455

(Received 28 May 1985)

The elastic scattering of 351-eV Auger electrons originating in the interfacial region is used to probe the structure of the Ag/Pd(001) interface. Polar-angle-resolved Auger-emission profiles and kinematical scattering calculations show that the mode of growth is epitaxial. Auger-electron diffraction in this intermediate energy range produces intensity maxima along low-index directions which result from simple near-neighbor forward scattering. The overall shapes of observed angular distributions are in good agreement with those predicted using kinematical scattering theory. This technique is shown to be sensitive to the local coordination of the emitting atom and is therefore useful for studying epitaxy at interfaces

Angle-resolved Auger and x-ray photoelectron spectroscopies are important tools for studying the atomic structure of abrupt metal-metal interfaces.^{1,2} Recent studies have emphasized the use of high-kinetic-energy electrons (~ 1000 eV) and have shown the existence of local diffraction-induced intensity maxima which accompany the establishment of low-index crystallographic directions in the overlayer. For these high-energy electrons, the forward focusing of scattered electron intensity has enabled a direct correspondence to be made between the appearance of a peak and the arrival of specific atoms in early stages of epitaxy. Likewise, kinematical or single-scattering cluster calculations have reproduced the experimental angular distributions very well.³ On the other hand, previous attempts to use intermediate-energy electrons (~ 300 eV) for such structural studies showed substantially less diffraction fine structure.² Indeed, in those studies it was concluded that fundamental differences in the nature of elastic electron-atom scattering at ~ 300 eV significantly reduces the utility of such measurements for studying epitaxy in metal-metal interfaces.³

In this paper, we show that angular intensity variations in intermediate-energy Auger emission are seen which correspond with the establishment of low-index directions in a fashion similar to that seen at higher energies. This result is useful because a number of Auger transitions occur at intermediate energies. We have performed polar-angle-resolved Auger-emission measurements on a metal-metal interface in which both substrate and overlay Auger emission occur at ~ 300 eV: Ag/Pd(001). Moreover, we find that kinematical scattering theory is useful in interpreting these anisotropies.

All measurements were performed utilizing an experimental system described in detail elsewhere.⁴ A single-crystal Pd(001) surface was cleaned and ordered by repeti-

tive cycles of Ar^+ bombardment and annealing at $\sim 600^\circ\text{C}$. The purity and structural quality of the surface were checked with Auger emission at a shallow, surface-enhancing collection angle and low-energy electron diffraction (LEED) I - V measurements.

Evaporations were monitored with a quartz crystal oscillator. High-purity Ag was evaporated from a tungsten basket in monolayer (ML) increments, referenced to the atom density of the substrate (1 ML = 2.25 Å). During evaporation, the chamber pressure rose from a base value of 4×10^{-11} to $(6-7) \times 10^{-11}$ Torr and remained in the mid- 10^{11} range during all measurements. At no point was any contaminant found on the surface during the two to three hour period required to collect LEED I - V curves and polar-angle Auger intensity profiles.

Auger excitation was accomplished using a 4-keV primary electron beam and incident currents of 0.1–0.5 μA . Polar intensity profiles were constructed from integrated $N(E)$ peak intensities collected every 2° from 0° (grazing emission) to 94° (90° is normal emission). The crystal was azimuthally oriented so that the (100) plane perpendicular to the surface bisected the 8° acceptance aperture of the energy analyzer.

In Fig. 1 we present polar-angle intensity profiles based on Pd MNN (326 eV) and Ag MNN (351 eV) Auger peaks as a function of Ag coverage. The Pd MNN profile for the clean surface shows local diffraction-induced maxima along low-index directions (indicated with arrows), as expected if forward scattering has any significant influence at ~ 300 eV. Moreover, this profile establishes a structural fingerprint for the well-ordered (100) surface of an fcc metal against which overlayer profiles can be compared. As coverage proceeds, all diffraction features remain stationary and simply attenuate uniformly with coverage. No new features appear, with the exception of a shoulder

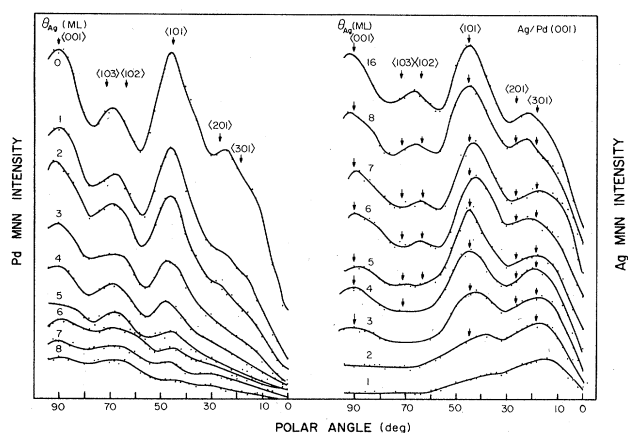


FIG. 1. Polar-angle intensity profiles associated with Pd MNN and Ag MNN Auger emission as a function of Ag coverage in monolayers. Arrows and Miller indices show the angles corresponding to low-index directions in the interface. For each coverage, arrows are placed in the Ag MNN profiles only if the associated low-index directions have been established by that coverage.

at 60° in the 6-ML curve, which does not appear in any other profile. This sort of behavior is expected if the mode of overlayer growth is epitaxial.

At 16 ML, the Ag MNN profile is essentially identical to the clean-surface Pd MNN profile. At this coverage, substrate signal attenuation is complete, rendering the surface "pure" Ag over a depth scale of ~ 3 mean free paths. The striking similarities between the two polar profiles establish that the mode of growth is indeed epitaxial, as expected in light of the similar lattice constants (3.88 \AA for Pd and 4.08 \AA for Ag).

Ag MNN polar profiles at lower coverages show that, as epitaxy proceeds, atoms occupying various lattice sites act as forward scatterers for electrons originating in underlying layers. In Fig. 1 we have placed arrows corresponding to low-index directions at the coverages for which those directions are established in the overlayer. For instance, as the second monolayer grows, emission from first-layer atoms should be enhanced at 45° , due to the zeroth order scattering by second-layer atoms. Thus, we place an arrow at 45° in the 2-ML polar profile. Indeed, the development of a feature at $\sim 40^\circ$ is evident in going from 1 to 2 ML. Similarly, atoms in the third layer will provide forward scatterers at 90° for first layer atoms. Thus a feature at 90° should develop as the third layer is built up but not before, and such is the case, as can be seen in Fig. 1. By 4 ML, a peak ought to appear at 72° , corresponding to the development of the $\langle 103 \rangle$ direction and by 5-ML emission at 63° should be enhanced due to the establishment of the $\langle 102 \rangle$ direction. However, it is not until 5 ML that a feature begins to develop in the range of 60° to 70° . This feature continues to grow with higher coverage. Maxima are also expected to appear at 18° by 2 ML ($\langle 301 \rangle$) and at 27° by 3 ML ($\langle 201 \rangle$). A weak feature appears at $\sim 20^\circ$ by 2 ML and remains at higher coverages. However, this feature is overshadowed

by a broad maximum at $\sim 14^\circ$ which is present by 1 ML.

In order to probe further into the structural details of the overlayer, we have performed theoretical calculations employing a kinematical scattering formalism which has been discussed in detail elsewhere.⁵ We have employed free-atom scattering factors interpolated from values tabulated by Gregory and Fink⁶ and Fink and Ingram.⁷ The inelastic mean free path⁸ and inner potential⁹ were taken to be 10 \AA and 14 eV , respectively. Lattice vibrations were simulated using tabulated Debye temperature data.¹⁰ A cluster size of 144 atoms per layer with two layers of Pd substrate and n layers of Ag where $n = 1, 2, 3, \dots, 8$ and 16 was found to be sufficiently large to obtain convergent results. The Pd lattice dimensions have been uniformly used throughout the cluster calculations.

In general, we find that the calculated intensity maxima along low-index directions are much larger than what is observed, due to the importance of multiple scattering at these intermediate energies. Moreover, the rate of growth of these features with coverage is calculated to be larger than the corresponding experimental rate. In Fig. 2, we compare theory with experiment, using a family of theoretical curves in the top panel and a corresponding family of experimental curves in the lower panel with the experimental intensity scale expanded by a factor of 3.

Although the absolute theoretical anisotropies are much larger than the corresponding experimental values, their relative intensities and peak positions are in generally good agreement. In both theory and experiment, we find for the higher coverages a large feature at 45° , corresponding to the $\langle 101 \rangle$ direction, a slightly weaker feature at 90° , coinciding with $\langle 001 \rangle$, and yet a weaker peak at $\sim 65^\circ$ – 75° corresponding to $\langle 103 \rangle$ and the $\langle 102 \rangle$ directions.

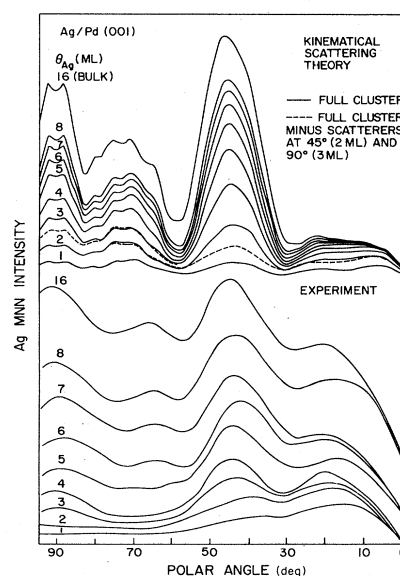


FIG. 2. Theoretical and experimental polar profiles as a function of coverage. The absolute theoretical diffraction intensities are much larger than those from experiment. Therefore, the intensity scale on the bottom panel has been increased by a factor of 3 for comparison with the top panel.

Using the data and calculations at low coverages, it is possible to assess the relative importance of simple forward scattering and more complicated interference effects at a kinetic energy of 351 eV. Looking first at the profiles for 1 ML, it is clear that diffraction features exist even though no second-layer forward scatterers are present. With the exception of forward scattering at 0° , such features are *not* present in an analogous theoretical polar profile for 1-ML Cu/Ni(001) in which Cu *LMM* Auger emission (917 eV) is used.³ In lowering the kinetic energy from 917 to 351 eV, it is found that the electron-atom scattering factors weaken and broaden in the forward direction and side and backscattering lobes develop.^{6,7} Thus the origin of these modulations at 1 ML appears to be interference effects caused by near-neighbor scattering in all directions and is not at all related to simple forward scattering.

This latter point can be easily shown by calculations using very small clusters, ranging from a single Ag atom to 49 Ag atoms in a single layer, supported by two Pd layers of 49 atoms each. Polar profiles resulting from these calculations are shown in Fig. 3 where we have plotted the Ag *MNN* intensities as anisotropies to demonstrate how the extent of interference grows with the number of atoms. For each curve, we express the cluster size using the notation $n \times m \times p \times q$ where $n \times m$ is the dimension of each layer, p is the number of Ag layers, and q is the number of Pd layers. A diagram of the surface is also provided to show the orientation of the emitter and scatterers with respect to the analyzer aperture. In profile

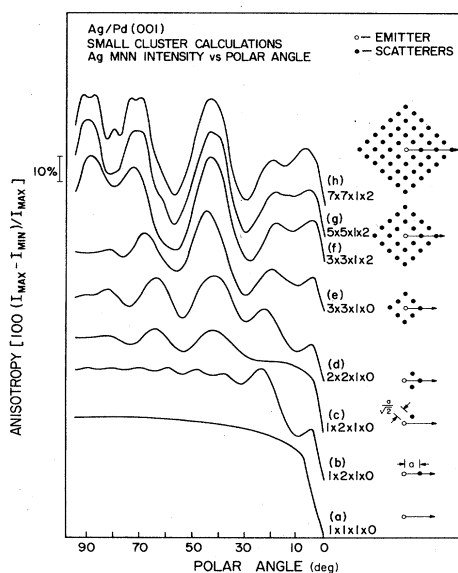


FIG. 3. Polar profiles resulting from small cluster calculations to show the origin of the interference effects at 1 ML. The cluster size is defined as $m \times n \times p \times q$ where $m \times n$ is the lateral dimensions per layer, p is the number of Ag layers, and q is the number of Pd layers. Also shown is a view of the cluster surface to indicate the relative orientations of the emitter and scatterers. The arrows lie in the detected emission plane and point in the direction of the spectrometer aperture.

a, we have a single Ag atom ($1 \times 1 \times 1 \times 0$). As expected, there is no diffraction modulation. In order to retain the effects of surface refraction, we have included in all calculations a surface potential barrier equal to the inner potential of Ag in the same way as was done in the full cluster calculations. Thus, the single-atom intensity is observed to fall off with decreasing polar angle as the reflection coefficient increases. In profile *b*, we have placed a second Ag atom in the emission plane, as shown to the right. We now observe oscillations in the scattering factor, modulated by the reflection coefficient. The critical angle for the Ag(001) surface is 11.3° so that we do not see the zeroth-order forward-scattering feature. In profile *c* we have placed a single Ag scatterer at 45° with respect to the emission plane. The diffraction fine structure is qualitatively different with major features appearing at polar angles of $\sim 45^\circ$ and $\sim 65^\circ$. As we expand the surface layer to 2×2 (curve *d*), we obtain the synthesis of curves *b* and *c*. No major changes in fine structure are induced by expanding the surface layer to 3×3 (curve *e*). However, the addition of two layers of Pd substrate (curve *f*) causes the appearance of a maximum at 90° which is due to backscattering and constructive interference with the primary wave. The de Broglie wavelength at 365 eV (measured kinetic energy plus inner potential) is 0.64 Å and is nearly an integral multiple of the assumed Ag to Pd interatomic spacing (3.88 Å) in the normal direction. Further expansion of the lateral dimension does not result in any significant change, as seen in profiles *g* and *h*. A small dip develops in the features at 90° and 70° for 7×7 atoms per layer (curve *h*), and this persists for higher coverages and larger cluster sizes (Fig. 2).

In order to assess the relative importance of simple zeroth-order forward scattering and these more complex interference effects at other coverages, we have performed full cluster calculations in which key forward scatterers have been removed. The resulting polar profiles are shown in Fig. 2 as dashed curves. For the 2-ML cluster, we have removed the forward-scattering second-layer atom at 45° with respect to the first-layer emitter. The result is a reduction in the 45° intensity by about a factor of 2. Similarly, removal of the 90° forward-scattering atom in the third layer causes a factor of 2 reduction in the feature at 90° . Thus, we have sensitivity to single-atom effects. It should be mentioned that the similarity in position of the forward-scattering features at coverages above 1 ML and the interference effects at 1 ML is entirely coincidental. Thus, the removal of key scattering atoms at 2 and 3 ML still leaves some intensity at forward-scattering angles due to interference effects.

In conclusion, we have used polar-angle-resolved Auger emission and a kinematical scattering formalism to probe the structure of a bimetallic interface in which the two metals have the same crystal structure and closely matched lattice constants. The growth mode is epitaxial, as judged by close similarities in diffraction-induced fine structure found in substrate and overlayer polar intensity profiles. Local intensity maxima are observed at polar angles corresponding to low-index directions. Furthermore, these intensity maxima appear with the addition of single atoms at lattice sites in the exit path of the emitted elec-

tron. The relative intensities and positions of the observed diffraction features are well reproduced by kinematical scattering theory, although the calculated absolute intensities are too large. The calculated anisotropies are shown to be due predominantly to simple forward scattering with minor contributions from more complex interference effects associated with side- and backscattering from near neighbors. Auger-electron diffraction in the energy range of 300–400 eV is shown to be a useful tool for studying

the early stages of epitaxial growth in bimetallic interfaces in that single-atom scattering can be observed and accounted for in terms of structure.

This work was supported by the National Science Foundation under Grants No. DMR-83-20242 (S.A.C. and S.B.A.) and No. DMR-82-16489 (J.H.W., Solid State Chemistry) and a grant from the Northwest Area Foundation of the Research Corporation.

¹W. F. Egelhoff, Jr., *J. Vac. Sci. Technol.* **A2**, 350 (1984).

²W. F. Egelhoff, Jr., *Phys. Rev. B* **30**, 1052 (1984).

³E. L. Bullock and C. S. Fadley, *Phys. Rev. B* **31**, 1212 (1985).

⁴S. A. Chambers and L. W. Swanson, *Surf. Sci.* **131**, 385 (1983).

⁵C. S. Fadley, in *Progress in Surface Science*, edited by S. G. Davison (Pergamon, New York, in press).

⁶D. Gregory and M. Fink, *At. Data Nucl. Data Tables* **14**, 39 (1974).

⁷M. Fink and J. Ingram, *At. Data* **4**, 129 (1972).

⁸M. P. Seah and W. A. Dench, *Surf. Int. Anal.* **1**, 2 (1979).

⁹G. A. Somorjai and H. H. Farrell, in *Advances in Chemical Physics*, edited by I. Prigogine and S. A. Rice (Wiley, New York, 1971); Vol. 20, p. 215.

¹⁰N. W. Ashcroft and D. D. Mermin, *Solid State Physics* (Holt, Rinehart and Winston, New York, 1976), p. 461.